Int. J. Heat Mass Transfer. Vol. 23, pp. 643–654.
Pergamon Press Ltd. 1980. Printed in Great Britain

DRY-OUT PHENOMENA IN GRAVITY-ASSIST HEAT PIPES WITH CAPILLARY FLOW

C. A. BUSSE
Joint Research Centre of the European Communities, 21020 Ispra, Italy
and
J. E. KEMME
Los Alamos Scientific Laboratory, Los Alamos, New Mexico 87545, U.S.A.

(*Received* 18 *May* 1979)

Abstract—The physical mechanism of the dry-out in gravity-assist heat pipes with capillary flow is analysed. Two contrary types of dry-out are shown to exist. The 'axial dry-out' arises from a lack of hydrostatic driving force and appears when the heat flux increases. For the 'azimuthal dry-out' it is just the opposite. The basic relations for the occurrence of these dry-outs are derived. Their evaluation is explained in an example. Methods for preventing the azimuthal dry-out are discussed. An Appendix contains some critical comments on the role of inertia forces and entrainment in heat pipes.

NOMENCLATURE

A, ratio of $\overline{w^2}$ to $\bar{w}^2$;
A_{eff}, effective cross section of the vapour channel;
B, function of Re_r, defined by equation (22);
d, inner diameter of the capillary structure;
d_h, hydraulic capillary diameter;
g, acceleration due to gravity;
l_h, evaporator length;
L, specific heat of vaporization of the working fluid;
N, number of liquid-flow channels;
P, vapour pressure;
P_c, capillary pressure;
P_{cm}, maximum capillary pressure;
$(P_{cm})_c$, maximum capillary pressure of the coarse part of a two-step graded wick;
$(P_{cm})_f$, maximum capillary pressure of the fine pore part of a two-step graded wick;
P_h, hydraulic pressure difference along the evaporator;
P_l, pressure in the liquid at the liquid–vapour interface;
$\mathbf{P}_l, \bar{P}_l$, lowest and highest value of P_l at any axial position x;
P_{lf}, P_l for completely filled capillaries;
$\mathbf{P}_{lf}, \bar{P}_{lf}$, lowest and highest value of P_{lf} at any axial position z;
P_{vl}, pressure on the liquid–vapour interface from the vapour side;
Q_m, axial heat flux in the transport zone;
Re_r, radial Reynolds number;
r_1, r_2, radii of curvature of the liquid–vapour interface;
v_n, vapour velocity normal to the interface;
w, axial vapour velocity;
$\bar{w}$, $\overline{w^2}$, average of w and w^2 over the cross section of the vapour channel;
z, axial coordinate;
z_D, axial coordinate of the dry point;
z_W, axial coordinate of the wet point.

Greek symbols

β, tilt angle of the heat pipe against the horizontal;
γ, surface tension of the working fluid;
ΔP_d, azimuthal dynamic liquid pressure drop;
ΔP_l, difference between P_l at wet and dry point;
ΔP_{vl}, difference between P_{vl} at dry and wet point;
η, viscosity of the vapour;
η_l, viscosity of the liquid;
λ, wavelength of capillary waves on a liquid–vapour interface;
ρ, density of the vapour;
ρ_l, density of the liquid.

1. INTRODUCTION

THE DRY-OUT of the capillary structure is a phenomenon of great concern for heat-pipe design as it can seriously deteriorate the heat-transfer characteristics of these devices. The purpose of this paper is to better understand the physical mechanism of dry-out phenomena and to put the conditions for their occurrence in mathematical form.

The analysis will deal with gravity-assist heat pipes having a capillary structure [1–4]. In gravity-assist heat pipes the presence of a capillary structure is not obligatory as in purely capillary-driven heat pipes. Nevertheless, most gravity-assist heat pipes do have a capillary structure in order to protect the liquid against the shear stress from the counter-flowing vapour and to help keep the surface of the evaporator wet.

Boiling will not be considered, nor will liquid flow outside the capillary structure. For this reason the heat pipes are, in general, assumed to contain no surplus liquid but just enough to saturate the capillary structure. However, a qualitative discussion will be included on the role of surplus liquid in the dry-out process and the problem of the transition from capillary flow into another flow mode.

To begin with, the condition for mechanical equilibrium at the liquid–vapour interface will be formulated (Section 2). After explaining how the dry-out conditions will be derived herefrom (Section 3), the pressure diagrams of the horizontal heat pipe (Section 4) and the gravity-assist heat pipe (Section 5) are discussed firstly for normal operation without a dry-out. Next, Sections 6 and 7 deal with the azimuthal dry-out and methods for preventing it. Section 8 contains a discussion of the axial dry-out and the basic equation for its occurrence. In the final section an example of how the dry-out heat flux can be derived herefrom is given.

2. MECHANICAL EQUILIBRIUM CONDITION

The dry-out is primarily a question of the mechanical equilibrium at the liquid–vapour interface, which consists of the balance of three pressures P_{vl}, P_l and P_c. P_{vl} is the pressure acting on the interface from the vapour side. It is the sum of the vapour pressure P and the kinetic reaction pressure ρv_n^2 of the evaporating- or condensing molecules

$$P_{vl} = P + \rho v_n^2. \tag{1}$$

P_l is the pressure acting on the interface from the liquid side. Similarly to (1), P_l is the sum of the liquid pressure and the kinetic reaction pressure of the liquid. However, as the liquid velocities are much smaller than the vapour velocities (except near the critical point), the kinetic reaction pressure of the liquid can generally be neglected and P_l identified directly with the liquid pressure. Finally P_c is the capillary pressure, which is generated in the interface. It depends on the surface tension γ and the curvature $1/r_1 + 1/r_2$ of the interface according to the classical Young–Laplace relation

$$P_c = \gamma(1/r_1 + 1/r_2). \tag{2}$$

P_c is counted positive when it acts in the same direction as P_l. Hence a concave curvature of the interface towards the vapour has to be described by positive radii of curvature, a convex curvature by negative ones. The mechanical equilibrium at the liquid–vapour interface then requires that

$$P_{vl} - P_l = P_c. \tag{3}$$

For given capillary geometry, surface tension and wetting angle, the capillary pressure P_c can vary within certain limits by a displacement of the interface. The upper limit P_{cm} of the capillary pressure is reached when the interface is at a position where its curvature becomes a maximum. P_{cm} can be calculated or measured relatively easily (apart from the problem of impurity enrichment at an evaporating meniscus, which results in uncertainties about the effective values of surface tension and wetting angle).

More problematical is the lower limit of the capillary pressure. One can design capillary openings where the minimum curvature of the interface and, hence, the minimum capillary pressure is negative. The menisci would then bulge towards the vapour side. This occurs, for example, if a cylindrical capillary ends in a flat surface and the wetting angle has finite values. The question is, however, whether such an arrangement of separated menisci would be stable under heat-pipe conditions, or whether, by vapour shear stress and condensation on the capillary structure, it would be transformed into a coherent liquid film on the capillary structure. Due to the relatively small curvature of such a film the corresponding minimum capillary pressure would then, in a first approximation, be zero. In the following analysis we shall assume such a minimum capillary pressure equal to zero. This is a safe estimate in the sense that it will lead easier to a dry-out than a negative minimum capillary pressure would do. Hence we have

$$0 \leq P_c \leq P_{cm}. \tag{4}$$

It should be noted that the assumption of a zero minimum capillary pressure implies that the heat pipe contains enough liquid to saturate the capillary structure. Saturation is the equilibrium between the liquid in the capillary structure and some surplus liquid. This means the menisci adjacent to the surplus liquid must have the same curvature as the surface of the latter. Saturation of the capillary structure, therefore, is synonymous with the fact that somewhere the liquid–vapour interface is flat like the surface of the surplus liquid or, if the curvature of the latter can be neglected, that somewhere the capillary pressure is zero.

Combining equations (3) and (4) it follows that at any liquid–vapour interface in the heat pipe

$$0 \leq P_{vl} - P_l \leq P_{cm}. \tag{5}$$

It will turn out that this condition essentially determines the dry-out.

3. THEORETICAL APPROACH OF THE DRY-OUT

For finding, theoretically, the dry-out conditions one could consider a similar proceeding as in the corresponding experiment. This would essentially mean assuming the heat pipe and its temperature (at one point) as given and changing the heat flux. The inconvenience of this approach is that both P_{vl} and P_l depend on the heat flux. This makes $P_{vl} - P_l$ a rather complex function of the heat flux.

A theoretically more transparent method, which will be used here, is to find the dry-out conditions by decreasing the surface tension γ, keeping heat flux, temperature and all other design- and operating parameters constant. To begin with, it is assumed that

the heat pipe is in a steady state and the capillary structure is completely filled with liquid. Then a stepwise decrease of the surface tension γ is made which causes, due to equation (2), a corresponding decrease of the capillary pressure P_c and, therefore, disturbs the mechanical equilibrium (3) at the liquid–vapour interface. This will entail no reaction on the vapour side, as the vapour-flow rate is determined by the constant heat flux. But there will be a reaction on the liquid side, which re-establishes the equilibrium (3), i.e. the liquid flow rate will change so that the decrease of P_c is balanced by a corresponding increase of P_l. This means the heat pipe enters a non-steady state where the unbalance between the vapour- and liquid-flow rates leads to a change of the liquid distribution in the heat pipe and, therefore, to a displacement of the liquid–vapour interface. This, in turn, can change both the curvature of the menisci and the liquid-flow resistance and thus modify P_c and P_l. The displacement, however, will generally have only a marginal effect on P_{vl} unless a dry-out occurs in the evaporator, which changes the axial vapour flow rate. The variation of P_c and P_l will then lead to further changes of the liquid flow rate, etc. The process may eventually lead to a new stationary state. For the present purpose it is not necessary to follow this complicated transition in detail. The main task will be to discover the new stationary state or to prove its non-existence.

The above description shows that approaching the dry-out by decreasing γ leaves P_{vl} essentially constant, which simplifies the discussion. Furthermore, it becomes apparent that it is important how the position of the interface, its curvature and the liquid flow resistance are interrelated. To specify these properties of the capillary structure the following definitions will be used:

Ungraded capillaries. A displacement of the liquid–vapour interface towards the inside of the capillary structure causes an increase of the curvature and of the liquid-flow resistance in such a way that at first the curvature rises from zero to maximum with negligible growth of the liquid flow resistance, and then the latter increases to infinity without further change of the curvature.

Graded capillaries. The same displacement of the interface causes an increase of the curvature and of the liquid flow resistance in such a way that the flow resistance becomes already infinite when the curvature reaches its maximum.

Interconnected capillaries. The liquid can flow in any direction. If the capillaries are not interconnected the liquid flow is essentially limited to one direction.

Here are some examples of capillary structures which, with some idealization, can be described by the above definitions:

Ungraded, interconnected: thick screen wicks.
Ungraded, not interconnected: deep U-grooves.
Graded, interconnected: coarse screen wick on top of a fine pore structure; crossing V-grooves (knurled surface).
Graded, not interconnected: V-grooves, shallow U-grooves.

Reference should also be made to capillary structures where the displacement of the interface towards the inside raises the flow resistance but decreases the curvature of the interface. One could call them 'inversely graded'. To this category belong, for example, all capillary structures of the artery type [5], as well as structures composed of a fine pore cover on top of a coarse capillary structure and grooves with increasing width towards the bottom. Inversely-graded capillary structures allow the simultaneous realization of low flow resistances and large capillary pressures and hence to carry large heat fluxes without the help of gravity [6]. However, they can also lead to stability problems and the priming of inversely-graded capillary structures under gravity is generally difficult. They have found little interest for terrestrial applications and will, therefore, no longer be considered here.

4. PRESSURE DIAGRAMS OF THE HORIZONTAL HEAT PIPE

After these preparatory remarks the dry-out mechanism will be investigated for a cylindrical heat pipe with a uniform ungraded interconnected capillary structure, tilted at an angle β with respect to the horizontal and consisting of evaporator, transport zone and condenser (Fig. 1). To begin with, the heat pipe is assumed to be in a steady state and P_{cm} larger than any value of $P_{vl} - P_l$ so that the capillary structure is completely filled with liquid. For this condition a plot will be made of P_{vl} and P_l over the whole liquid–vapour interface. It is most convenient to plot P_{vl} and P_l over the axial coordinate z of the interface and to use the azimuthal position of the interface as a parameter. A horizontal heat pipe will be considered first ($\beta = 0$).

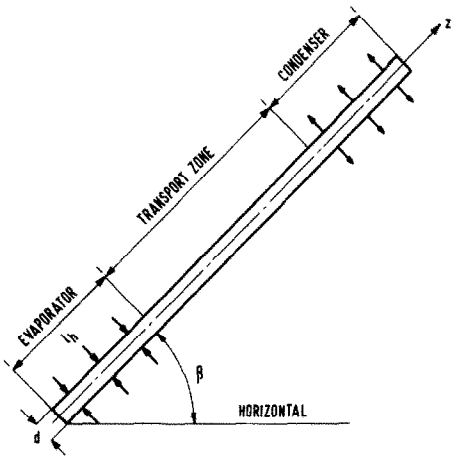

FIG. 1. Heat pipe with coordinates.

For relatively long heat pipes the vapour pressure can be assumed to be constant over the cross section of the pipe [7]. Then the vapour pressure P can be presented by a single curve. For radial Reynolds numbers $Re_r \ll 1$, i.e. small heat fluxes, the vapour flow is essentially subject to viscous forces only, so that the vapour pressure shows a steady drop along the heat pipe (dashed curve in Fig. 2a). For higher heat fluxes, more precisely for $Re_r \gg 1$ (see Appendix 1), the vapour flow is dominated by inertia forces, which lead to a partial pressure recovery in the condenser and to a change of the slope of the vapour-pressure curves at both ends of the transport zone [7] (dashed curve in Fig. 2b.). The absolute position of the vapour-pressure curve in the pressure diagram is determined by the temperature at one point of the interface and the (approximate) thermodynamic equilibrium between vapour and liquid. Adding to P both in the evaporator and condenser the kinetic-reaction pressure correction ρv_n^2 one obtains the P_{vl} curve (solid line in Figs. 2a and 2b).

In contrast to P_{vl}, the liquid pressure P_l depends on the azimuthal position because of hydrostatic forces. Hence, there is an infinite number of P_l curves. They lie within the hatched band in Figs. 2a and 2b. If there is no azimuthal flow and, therefore, no dynamic azimuthal pressure gradient, the width of the P_l band will be equal to the hydrostatic pressure $\rho_l g d$ over the diameter d of the vapour channel. If there is a downward azimuthal flow, this superimposes in flow direction a negative pressure gradient from viscous forces on the positive hydrostatic pressure gradient and thus decreases the width of the band. Correspondingly, an upward azimuthal flow would increase the band width. If the dynamic azimuthal pressure gradients can be neglected the upper edge of the P_l band corresponds in each case to the lowest point of the cross-section, the lower edge to the highest one.

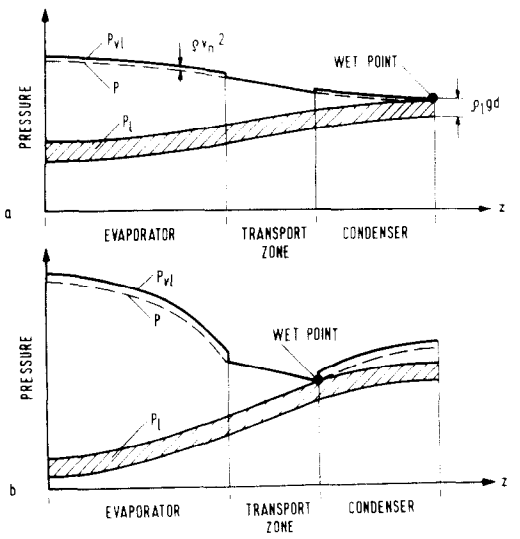

FIG. 2. Pressure diagrams of horizontal heat pipes at different heat fluxes (schematic).

In the liquid flow the inertia forces can generally be neglected (for exceptions see Appendix 1). Therefore, similar to the vapour-pressure curve P in Fig. 2a, the P_l band shows a steady decrease in flow direction. The absolute position of the P_l band in the diagram is determined by the LHS of condition (5) together with the assumption of a saturated capillary structure: condition (5) excludes that P_l is larger than P_{vl}, and saturation means, as explained above, that there is at least one point with $P_c = 0$ and, therefore, $P_{vl} = P_l$. So the band of the P_l curves lies below the P_{vl} curve and touches the latter at least in one point

These touching points will turn out to be important. Following a proposal of van Andel [8] we call them 'wet points'. If the heat pipe contains surplus liquid it will tend to be accumulated at such wet points. Figures 2a and 2b each show one wet point; they occur in both cases at the upper edge of the P_l band, once at the end and once at the beginning of the condenser.

The curvature of the liquid–vapour interface adjusts itself in such a way that, according to equation (3), the capillary pressure P_c becomes equal to the difference between P_{vl} and P_l. The maximum curvature is seen to occur at the top of the beginning of the evaporator.

5. PRESSURE DIAGRAMS OF THE GRAVITY-ASSIST HEAT PIPE

Now if the horizontal heat pipe of the preceding section is tilted to a gravity-assist position, the P_{vl} curve will not change, but the hydrostatic force in z direction will superimpose a negative pressure gradient on the positive gradient of the liquid-pressure curves in Figs. 2a and 2b. As a result the slope of the P_l band will become less positive or even negative. The latter case is shown schematically for several heat fluxes in Fig. 3.

Figure 3a represents the limiting case of a zero heat flux, i.e. zero dynamic pressure gradients. Then the P_{vl} curve is simply a horizontal line and the liquid pressure is identical with the hydrostatic pressure. So the P_l band is straight and has a constant width of $\rho_l g d \cos\beta$ corresponding to the hydrostatic pressure difference over the diameter of the vapour channel. In contrast to Fig. 2 the wet point now occurs at the beginning of the evaporator.

Figures 3b and d show the variation of the pressure diagram of Fig. 3a with rising heat flux. The P_{vl} curve will transform at first into a curve as in Fig. 2a (not shown in Fig. 3). Then, at $Re_r \gg 1$, it assumes the shape of that in Fig. 2b. The absolute steepness of the different parts of the P_{vl} curve increases with the heat flux. The liquid flow superimposes a positive dynamic-pressure-gradient on the negative hydrostatic gradient so that the hatched P_l band becomes less steep with increasing heat flux (the dashed line repeats for comparison the purely hydrostatic gradient of Fig. 3a). As a result of these variations the wet point is seen to shift from the beginning of the evaporator (Figs. 3a and 3b) to the end of the evaporator (Fig. 3c) and finally to the beginning of the condenser (Fig. 3d). Thus at

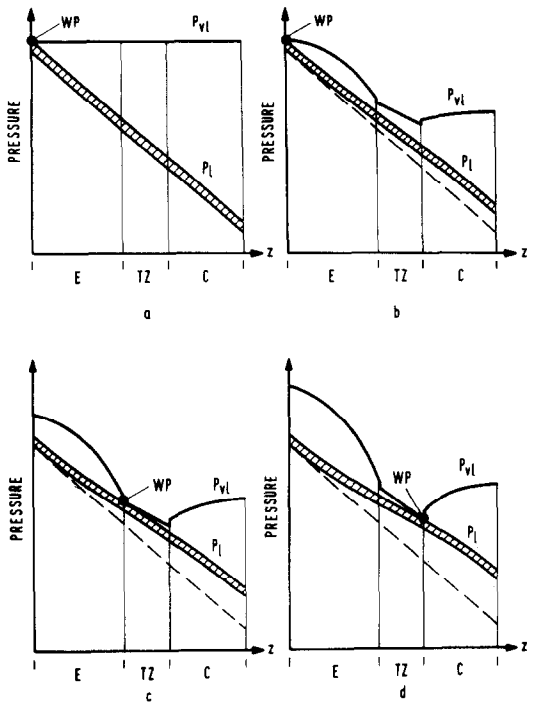

FIG. 3. Pressure diagrams of gravity-assist heat pipes at different heat fluxes (schematic). E = evaporator, TZ = transport zone, C = condenser.

sufficiently high heat fluxes the pressure diagram of the gravity-assist heat pipe begins to show similarity with the diagram of a horizontal heat pipe shown in Fig. 2b.

The most striking difference between Figs. 2 and 3 is the fact that the pressure diagram of the gravity-assist heat pipe can have a wet point at the beginning of the evaporator. This corresponds to the familiar observation that surplus liquid can form a pool at the lower end of a gravity-assist heat pipe. Another interesting fact is that the P_{vl} curve and the P_l band may both converge or diverge in the z direction. In the examples of Fig. 3 there can be as many as two zones of diverging and one of converging in the same heat pipe. A zone of converging means that the liquid could not return against the pressure from the vapour without the help of the capillary force. It therefore, signalizes a lack of hydrostatic driving force. Similarly, a diverging of P_{vl} and P_l in the z direction indicates a surplus of hydrostatic driving force. So one has to deal with two physically quite different transport situations. In previous theoretical work on transport limitations in capillary-driven heat pipes the attention was directed only towards the zone of converging. Figure 2 shows that for capillary-driven heat pipes, in fact, the converging dominates. In contrast to this, it appears from Fig. 3 that gravity-assist heat pipes can also have zones with strong diverging, especially at low heat fluxes. The following analysis will show that both the converging and diverging of P_{vl} and P_l can lead to a dry-out, but of very different nature.

6. THE AZIMUTHAL DRY-OUT

The dry-out will now be approached by a stepwise decrease of γ, which is accompanied by a corresponding decrease of P_{cm}. The discussion will be based on the pressure diagram of Fig. 3b, showing a wet point at the beginning of the evaporator, two zones of diverging P_{vl} and P_l and one zone of converging.

As long as P_{cm} remains everywhere larger than $P_{vl} - P_l$ the new stationary state, which the heat pipe will reach after a decrease of γ, can easily be indicated. It is characterized by an increased curvature of the menisci and the same pressure diagram as before. The increased curvature cancels the decrease of γ and leads to the old values of P_c. P_{vl} remains constant in any case, as explained in Section 3. Finally P_l does not change because, for the assumed ungraded capillary structure, the change of curvature of the menisci has a negligible effect on the liquid-flow resistance. The new stationary state shows no dry-out so far.

Upon further decrease of γ resp. P_{cm}, namely when P_{cm} becomes smaller than the maximum of $P_{vl} - P_l$, a second type of transition appears. This happens in Fig. 3b at first at the right hand side of the pressure diagram. The condition (5) now requires a decrease of $P_{vl} - P_l$, hence a change of the P_l band. There exists, in fact, a corresponding stationary state, which is characterized by menisci receded into the capillary structure. The receding increases the liquid flow resistance and, therefore, the liquid pressure gradient in z direction. This means that the diverging of P_{vl} and P_l and hence the difference $P_{vl} - P_l$ becomes smaller. The degree of receding depends on how much $P_{vl} - P_l$ has to be decreased. For the assumed ungraded structure the capillary pressure P_c and, therefore, also $P_{vl} - P_l$ has the same value P_{cm} for all receded menisci independent of how deep they recede into the capillary structure. Therefore, all receded menisci are presented by a single P_l curve, which runs parallel to the P_{vl} curve at a distance equal in value of P_{cm}. All unreceded menisci, for which $P_c < P_{cm}$, are accordingly represented by P_l curves above that for the receded menisci. So the lower edge of the modified P_l band runs parallel to the P_{vl} curve at a distance corresponding to P_{cm} and the width of the P_l band is decreased to the value of the maximum azimuthal-pressure difference between the unreceded menisci of a cross section.

Figure 4 shows the pressure diagram of Fig. 3b with two additional pressure bands, P_l' and P_l'' for the receded menisci, which correspond to two different values of P_{cm}. The original P_l band of Fig. 3b describing the liquid pressure for the unreceded state of the menisci is now called P_{lf}. The P_l' band has only a single zone with receded menisci. It begins at z_3 in the second zone of diverging, where the spacing between the P_{vl} curve and the lower edge of the P_{lf} band becomes larger in value than the maximum capillary pressure and it continues to the end of the condenser. The P_l'' band corresponds to a still smaller value of P_{cm} and shows two zones with receded menisci. This phenomenon is caused by the fact that the diverging of P_{vl}

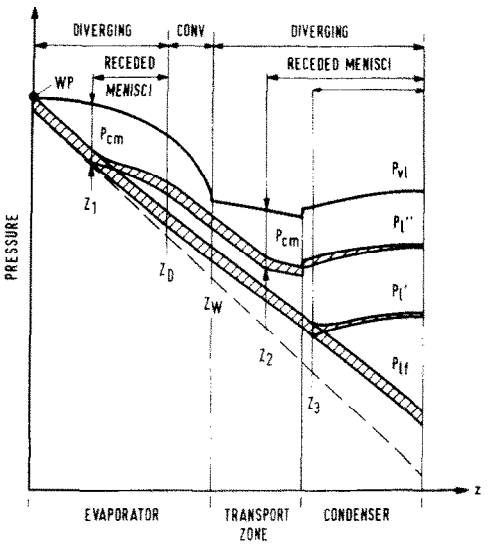

FIG. 4. Pressure diagram for an azimuthal dry-out (schematic).

and the P_{lf} band is interrupted by a zone of converging extending from z_D to z_W. The first receding of the menisci begins at z_1. There the lower edge of the P_l'' band starts to run parallel to the P_{vl} curve at a distance corresponding to P_{cm}. This, however, cannot continue beyond z_D because then a liquid pressure band parallel to P_{vl} would run steeper than the original P_{lf} band, which is impossible because the liquid flow resistance cannot be smaller than in the case of unreceded menisci. Hence, from z_D on the menisci are no longer receded and the P_l'' band again assumes the slope of the original P_{lf} band. So the P_l'' band runs parallel to P_{lf} through the whole zone of converging up to the point z_2 in the next zone of diverging, where once again the spacing between P_{vl} and the lower edge of the P_l'' band would become larger in value than P_{cm} if the P_l'' band continues parallel to P_{lf}. There the second zone of the receded menisci begins, extending to the end of the condenser just as in the example P_l'.

The question remains whether in the new steady state some of the menisci may have receded down to the bottom of the capillary structure, so that a dry-out exists. This can in fact happen. It was pointed out that any receded meniscus is represented by the lower edge of the P_l band. So the liquid pressure at all receded menisci on the same circumference has the same value. This is impossible for menisci which are situated at different elevations, unless the hydrostatic pressure differences between them is compensated by the dynamic pressure gradient of a downward azimuthal flow. Such a compensation evidently occurs in the condenser where the continuous generation of liquid all over the capillary structure prevents a dry-out. So there is a continuous azimuthal downward flow in the condenser, and the menisci recede only until the dynamic- and hydrostatic-pressure gradient in the azimuthal direction balance each other. However, if there is no downward azimuthal liquid flow or even an upwards one, as is likely to happen in the evaporator, the receding of the menisci will lead to a dry-out of the upper part of the circumference and the liquid flow will be concentrated on the completely filled lower part of the capillary structure.

This 'azimuthal dry-out' is purely a question of the azimuthal distribution of the liquid flow and not of any lack of total axial liquid return. In principle, the heat pipe can then be operated stationarily without any change of the axial heat flux, provided that the heating is concentrated on the remaining wet region of each circumference. This outcome is not surprising, if one looks at the origin of the azimuthal dry-out, namely the diverging of P_{vl} and P_{lf}, which means an excess of hydrostatic driving force.

As long as the azimuthal dry-out occurs outside the evaporator, it does not affect the heat transfer. Therefore, the next question is: when will the azimuthal dry-out occur in the evaporator? The answer is evident from Fig. 4: the difference $P_{vl} - P_{lf}$ must increase in the evaporator and on the right hand side of the wet point to more than P_{cm}. Figure 3 shows that this gets easier as the heat flux becomes smaller. The azimuthal dry-out, therefore, is a phenomenon which is most likely to occur during start-up and which can disappear at higher heat fluxes, a behaviour just opposite to the familiar dry-out of capillary-driven heat pipes.

7. PREVENTING THE AZIMUTHAL DRY-OUT

When the heat pipe is operated with constant-temperature heating, an azimuthal dry-out causes an automatic shifting of the whole heat input to the remaining wet part of the evaporator. In this case the azimuthal dry-out may be of no concern, as it only results in a certain decrease of the heat-transfer coefficient. For constant-power heating, however, the azimuthal dry-out leads to a hot spot and eventually also to a rewetting problem at higher heat fluxes, when the dry-out should, in theory, disappear. So the question arises how an azimuthal dry-out could be prevented.

For the ungraded interconnected capillary structure the answer is shown by Fig. 3a: the maximum capillary pressure has to be larger than the maximum hydrostatic pressure difference in the evaporator, i.e.

$$P_{cm} \geq \rho_l g(l_h \sin\beta + d\cos\beta). \tag{6}$$

In other words, the static capillary rise must exceed the highest point of the evaporator, a condition, which for larger elevations in the evaporator, may be difficult to satisfy.

Another possibility to prevent azimuthal dry-outs is to use a different capillary structure. One could think of non-interconnected structures, such as axially running grooves without any azimuthal connection. This evidently impedes the azimuthal redistribution of the axial liquid flow, which is necessary for the occurrence of an azimuthal dry-out. But then another problem appears, namely that from each groove only the

amount of liquid which is condensed into it can be evaporated. Hence for a non-interconnected capillary structure-heating and cooling must be balanced for each groove in order to avoid a dry-out of the beginning of a groove. This is difficult to achieve even in the seemingly simple case of axially symmetric heating and cooling, because the axial symmetry can be disturbed by a leakage of liquid from the upper to the lower grooves [9]. An azimuthal connection of the grooves at the beginning of the evaporator brings some help by allowing a liquid flow, which can compensate heating–cooling imbalances or azimuthal leakage. This method is efficient for horizontal heat pipes of not too large diameter, but it may be of no help for long gravity-assist heat pipes where the compensating liquid flow would have to overcome important gravity effects.

A more promising method of preventing azimuthal dry-outs is the use of interconnected graded capillary structures. The grading will allow the elimination of the weak point of the ungraded capillary structure, which is that the capillary pressure cannot vary azimuthal when the menisci are receded. This will be illustrated by an example. Let us consider an interconnected capillary structure with a two-step grading, which consists of a coarse wick on top of a fine-pore wick. The task of the coarse wick is the axial liquid transport, that of the fine-pore wick the azimuthal liquid distribution in the region of the azimuthal dry-out of the coarse wick. Figure 5 shows schematically the corresponding pressure diagram in the evaporator. For simplicity the vapour pressure drop has been neglected, i.e. the P_{vl} curve is a horizontal line. The upper part of the hatched area gives the liquid pressure in the wet part of the coarse wick. At z_1 the lower edge of the P_l band reaches the maximum possible distance from the P_{vl} curve, given by the value of the maximum capillary pressure $(P_{cm})_c$ of the coarse wick. This is the beginning of the azimuthal dry-out of the coarse wick, which raises the axial liquid-flow resistance until the lower edge of the P_l band of the coarse wick runs parallel to the P_{vl} curve. The band width, representing the azimuthal liquid-pressure difference over the remaining wet part of the coarse wick, is correspondingly reduced.

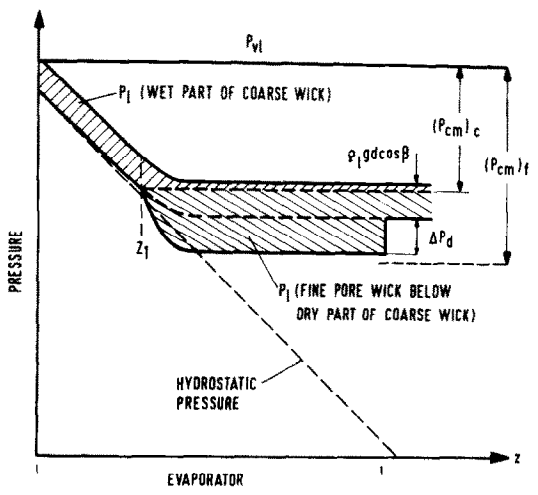

FIG. 5. Pressure diagram for a two-step graded capillary structure (schematic).

In the dry part of the coarse wick the menisci are receded into the fine-pore wick. The lower part of the hatched area gives the liquid pressure in this region. The figure shows the increase of the width of the P_l band by the dynamic pressure drop ΔP_d from the upward azimuthal flow in the fine-pore wick. To keep the entire evaporator wet the maximum capillary pressure $(P_{cm})_f$ of the fine-pore wick must be larger than any difference $P_{vl} - P_l$ in the evaporator. Figure 5 shows that for this purpose it is sufficient to make

$$(P_{cm})_f \geq (P_{cm})_c + \rho_l g d \cos\beta + \Delta P_d. \tag{7}$$

This condition is easier to fulfil than condition (6) because it is independent of the evaporator length l_h. Therefore, even for very long evaporators, only a relatively small capillary pressure $(P_{cm})_f$ is necessary.

It must be noted that in the foregoing consideration the fine-pore wick has tacitly been assumed to have an infinitely-large axial-flow resistance. If it has only a finite resistance, there will be a heat flux below which even a complete azimuthal dry-out of the coarse wick could not produce the required increase of the axial liquid-flow resistance. Then also an azimuthal dry-out of the fine-pore wick would occur. In order to limit this dry-out to very low heat fluxes, where the correspondingly low heating rates may hardly cause an inacceptable superheating of the evaporator, care should be taken to make the fine-pore wick no thicker than required by the azimuthal transport requirements.

8. THE AXIAL DRY-OUT

Let us now return to Fig. 4 and examine the consequences of a further decrease of γ resp. P_{cm}. The heat input is assumed to be concentrated on the wet region of each circumference. This leaves the P_{vl} curve constant, apart from a change in the correction ρv_n^2 in the region of the azimuthal dry-out.

At first there is no qualitative variation. The P_l band rises further and the zones with receded menisci extend in length. This happens until the upper edge of the P_l band touches the P_{vl} curve at z_W thus creating a second wet point as shown in Fig. 6. Then

$$\Delta P_{vl} + \Delta P_l = P_{cm} \tag{8}$$

where $-\Delta P_l$ is the liquid-pressure difference between the point DP and WP of the liquid–vapour interface and ΔP_{vl} the corresponding pressure difference on the vapour side of these two points. DP will be called 'dry point' in contrast with the wet point WP (the pressure balance at the dry point will in fact be found to determine a dry-out which, however, occurs generally at another location; the term 'dry point' must, therefore, not be misinterpreted).

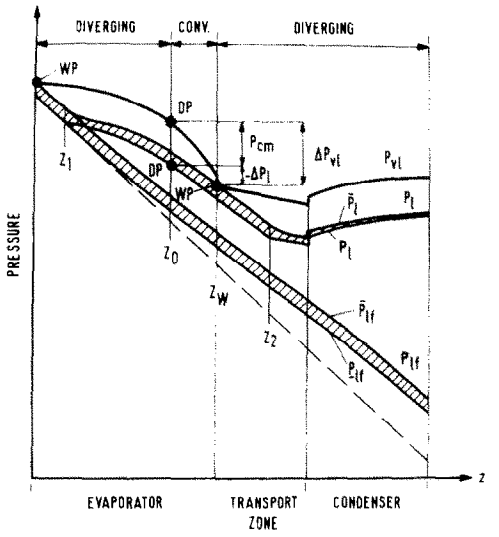

FIG. 6. Pressure diagram for an axial dry-out (schematic).

Now the LHS of equation (5) excludes a further rise of the P_l band at z_W. Upon further decrease of P_{cm} the condition (5) could still be satisfied in the two zones of diverging P_{vl} and P_l by continued receding of the menisci, but a difficulty arises in the zone of convergence between z_D and z_W. Condition (5) requires a rise of P_l in this zone, beginning with the lower edge of the P_l band at z_D. In the stationary state this could only be achieved by a decrease of the axial liquid-flow resistance between z_D and z_W. This is evidently impossible for capillary flow, because the capillary structure in this zone is already completely filled with liquid and the flow resistance is, therefore, at its minimum. A decrease of the liquid-flow resistance can only be achieved by creating an additional flow path outside of the capillary structure, so there no longer exists a stationary state in the capillary flow mode when P_{cm} becomes smaller than the value given by equation (8).

Now the question is: where will the non-steady state lead to? In Fig. 6 a decrease of γ and the corresponding rise of the P_l band make the liquid pressure drop from z_D to z_W larger. This means that less liquid is transported through this zone than before. Therefore, further downstream from z_D, there will be a decrease of the liquid inventory. In detail the consequences depend on whether or not there is a pool of surplus liquid at the bottom of the heat pipe. No pool will exist if the heat pipe either contains no surplus liquid or if there is no wet point at the beginning of the evaporator, where the surplus liquid could be accumulated. This happens for horizontal heat pipes (see Fig. 2) but also for gravity-assist heat pipes with a pressure diagram as in Fig. 3c or 3d. In all these cases the lack of axial liquid return will result in a dry-out at the downstream end of the liquid flow, i.e. usually the beginning of the evaporator. This will be called an 'axial dry-out'. It is in several respects just the opposite of the azimuthal dry-out: the axial dry-out is caused by the converging of P_{vl} and P_l and not by the diverging, this means by a lack of hydrostatic driving force instead of an excess; its occurrence is promoted by an increase of the heat flux rather than by a decrease (see Fig. 3) and the heat pipe can no longer be operated stationary without a change of the axial heat flux.

It the heat pipe contains surplus liquid and has a wet point at the beginning of the evaporator, as in the pressure diagram of Fig. 6, then a pool will exist. In this case the part of the evaporator which is no longer reached by the reduced liquid return flow, will begin to draw liquid from the pool. So the transition into a non-steady state will reveal itself at first as a lowering of the level of the pool. The volume of liquid, which disappears from the pool, will be accumulated at the other wet point at z_W. Now the question arises: can this liquid run down on the outside of the capillary structure? The analysis of this flooding problem is beyond the scope of this paper. Only a few generic remarks shall be added in order to show some basic alternatives.

It is easy to specify a case when no flooding is possible, namely when the hydrostatic force is not sufficient to drive the liquid down against the rising pressure on the vapour side, even without the retarding action of vapour shear stress and liquid viscosity. This means

$$\rho_l g \sin\beta < -\frac{\mathrm{d}P_{vl}}{\mathrm{d}z}. \tag{9}$$

If this condition is satisfied at the liquid downstream side of z_W, then the accumulating surplus liquid at z_W cannot run down again. So the non-steady state will lead to a dry-out as soon as the pool has disappeared or its level has dropped too far down for drawing up enough liquid.

Evaluation of equation (9) shows that the heat fluxes required for this case can be fairly high. So the possibility has to be considered that condition (9) is not satisfied. Then flooding becomes a quantitative question of the retarding action of the vapour shear stress. If the film of surplus liquid is thin, vapour shear produces a large retarding pressure gradient and prevents flooding. With continued transfer of the pool to z_W and thus increasing film thickness the retarding pressure gradient at first becomes smaller. But then additional retarding effects arise from the reduction of the cross section for the vapour flow and the instability of the liquid surface. The latter can result in stripping of droplets, which are carried upwards by the vapour. While such an entrainment of liquid has probably no influence on the axial dry-out of capillary-driven heat pipes, it may play an important role in gravity-assist heat pipes (see Appendix 2).

In any case it cannot be excluded that flooding may occur if condition (9) is not satisfied. Then the non-steady state will not lead to a dry-out but instead, after a certain quantity of the pool has been transferred, to a new stationary state characterized by a mixture of capillary flow and free flow outside the capillaries.

9. AXIAL DRY-OUT HEAT FLUX

The condition for the axial dry-out in the capillary flow mode is given by equation (8). It is formally identical with the familiar basic equation of capillary-driven heat pipes. The novelty lies in the definition of the pressure differences ΔP_{vl} and ΔP_l. From Fig. 6

$$\Delta P_{vl} = P_{vl}(z_D) - P_{vl}(z_W), \tag{10}$$

$$-\Delta P_l = \mathbf{P}_l(z_D) - \bar{P}_l(z_W). \tag{11}$$

The calculation of these pressure differences is not as straightforward as for capillary-driven heat pipes, because it requires the location of the dry- and the wet points and consideration of the influence of menisci receding on the P_l band.

For ungraded interconnected capillary structures this task can be greatly simplified by the assumption that the P_l band between z_D and z_W in Fig. 6 is a parallel displaced P_{lf} band. This is not exactly true because the receding of the menisci will not be without influence on the liquid flow near the ends of the zone of unreceded menisci between z_D and z_2, but it can serve as a first approximation. Then equation (11) becomes

$$-\Delta P_l = \mathbf{P}_{lf}(z_D) - \bar{P}_{lf}(z_W) \tag{12}$$

where P_{lf} can easily be calculated. Furthermore, Fig. 6 shows that the axial coordinates z_D and z_W are then determined by the beginning of the converging of P_{vl} and $\mathbf{P}_{lf}$ and by the end of the converging of P_{vl} and $\bar{P}_{lf}$, respectively. This rule holds when there is only a single zone of converging. It can, however, without too much difficulty be extended to more complex heat pipes than those considered here, where more than one zone of converging P_{vl} and P_{lf} may exist. So, expressing P_{vl}, $\bar{P}_{lf}$ and $\mathbf{P}_{lf}$ as functions of the maximum heat flux Q_m and the axial coordinate z, then determining z_D and z_W from the above rule and ΔP_{vl} and ΔP_l respectively from equations (10) and (12), one obtains from (8) the heat flux, Q_m, at the axial dry-out limit.

For graded interconnected capillaries with the two-step grading described in Section 7, one can proceed exactly as above, considering only the coarse part of the wick. For a general grading, however, the procedure becomes more complex. Equations (8), (10) and (11) are evidently also valid for this case. As the liquid-flow resistance now changes with the curvature of the menisci and hence with the absolute position of the P_l curves in the pressure diagram, it is necessary, for the calculation of P_l, to know the wet point already. This may require an iterative procedure. Figure 3 shows that for small heat fluxes $z_W = 0$. This case is, however, of no interest as an axial dry-out can only occur when the wet point lies at the end of the zone of converging P_v and P_{vl} and hence necessarily at some $z_W > 0$, as shown by Figs. 3c, d and the limiting case of Fig. 6, with both a wet point at $z = 0$ and $z_W > 0$. z_D and z_W are now determined, therefore, by the beginning of the converging of P_{vl} and $\mathbf{P}_l$ and by the end of the converging of P_{vl} and $\bar{P}_l$, respectively, together with the condition that a wet point must exist at z_W. Again this rule is limited to cases with a single zone of converging.

The mathematical details of the evaluation of the foregoing equations depend strongly on the physical character of the respective flows and will be presented elsewhere. Just as an example a relatively simple case which has recently been discussed in the literature [2, 10] will be considered here. This case is characterized by the following assumptions:

(1) Constant heating rate, i.e. the heat flux Q increases in the evaporator linearly with z

$$Q = Q_m \frac{z}{l_h}. \tag{13}$$

(2) Negligible dynamic liquid-pressure drop and vertical operation ($\beta = 90°$), i.e.

$$\bar{P}_{lf} = \mathbf{P}_{lf} = P_{lf} \tag{14}$$

and

$$\frac{\mathrm{d}}{\mathrm{d}z} P_{lf} = -\rho_l g. \tag{15}$$

(3) Negligible kinetic reaction pressure ρv_n^2 and dominating inertia forces in the vapour.

The latter assumption necessitates that the radial Reynolds number is large compared to one, i.e.

$$Re_r = \frac{1}{2\pi\eta L} \frac{Q_m}{l_h} \gg 1. \tag{16}$$

Then for incompressible flow

$$\frac{\mathrm{d}}{\mathrm{d}z} P_{vl} = -\frac{A}{A_{\mathrm{eff}}^2 \rho L^2} \frac{\mathrm{d}Q^2}{\mathrm{d}z} \tag{17}$$

where A is a correction of the order of 1 defined by

$$A = \frac{\overline{w^2}}{\overline{w}^2} \tag{18}$$

and given explicitly in [11].

(4) Wet point at the end of the evaporator as in Figs. 3c or 6, i.e.

$$z_W = l_h. \tag{19}$$

This necessitates that the vapour-pressure gradient at the beginning of the transport zone is larger than the gradient of P_{lf}. Hence follows with equation (15)

$$\frac{\mathrm{d}P_{vl}}{\mathrm{d}z} > -\rho_l g. \tag{20}$$

This can be written

$$\frac{8\pi B}{A_{\mathrm{eff}}^2} \frac{\eta Q_m}{\rho L} < \rho_l g \tag{21}$$

where B is a correction between 1 and 1.66, which depends on the radial Reynolds number of the heating zone according to the approximate relation [7]

$$B = 1 + \frac{3.3\, Re_r}{18 + 5\, Re_r}. \tag{22}$$

Both assumptions (16) and (21) have to be verified *a posteriori* with the calculated heat flux Q_m.

According to the above given rule the dry point is determined by

$$\left[\frac{\mathrm{d}}{\mathrm{d}z}(P_{vl} - P_{lf})\right]_{z=z_D} = 0. \tag{23}$$

Hence follows with (17), (15) and (13)

$$-\frac{A}{A_{\mathrm{eff}}^2 \rho L^2} Q_m^2 \frac{2z_D}{l_h^2} + \rho_l g = 0. \tag{24}$$

This equation gives the axial coordinate z_D of the dry point as a function of Q_m. Furthermore, one obtains from equation (10) by integration of (17), making use of equations (13) and (19)

$$\Delta P_{vl} = \frac{A}{A_{\mathrm{eff}}^2 \rho L^2} Q_m^2 \left(1 - \frac{z_D^2}{l_h^2}\right). \tag{25}$$

Similarly it follows from (12) with equations (15), (14) and (19)

$$\Delta P_l = -\rho_l g l_h \left(1 - \frac{z_D}{l_h}\right). \tag{26}$$

Inserting equations (25), (26) and z_D from equation (24) into (8) and resolving for Q_m, one finds

$$Q_m = A_{\mathrm{eff}} L \left(\frac{\rho}{A}\left[\frac{P_h}{2} + \frac{P_{cm}}{2} + \tfrac{1}{2}\sqrt{P_{cm}^2 + 2P_{cm}P_h}\right]\right)^{1/2} \tag{27}$$

where P_h is the hydraulic pressure difference along the evaporator, i.e.

$$P_h = \rho_l g l_h. \tag{28}$$

The result (27) is rather close to the earlier approximate formula [2, 10] given by

$$Q_m = A_{\mathrm{eff}} L \left(\frac{\rho}{A}\left[\frac{P_h}{2} + P_{cm}\right]\right)^{1/2} \tag{29}$$

The difference between equations (27) and (29) consists in the $P_{cm}P_h$-term on the RHS of (27), which disappears both for $P_{cm} = 0$ and $P_h = 0$. The maximum deviation occurs for $P_h = 4P_{cm}$, where equation (29) gives a heat flux 13% too low.

10. CONCLUSIONS

There are two types of dry-out, which can occur in gravity-assist heat pipes with capillary flow. They are in several aspects contrary to each other. The 'azimuthal dry-out' is caused by an excess of hydrostatic driving force. It is characterized by a concentration of the liquid flow on the lower part of the cross section without any lack of axial liquid return. The heat pipe can then still be operated stationary without any change of the axial heat flux, concentrating the heating on the wet part of each circumference. The azimuthal dry-out appears with decreasing heat flux. The best way to prevent azimuthal dry-outs seems to be the use of graded capillary structures.

In contrast with this, the 'axial dry-out' is caused by a lack of hydrostatic driving force. It appears with increasing heat flux as a result of the transition into a non-steady state, which is characterized by insufficient axial liquid return. A return from this non-steady state to stationary operation is no more possible without changing the axial heat flux, except for certain cases where a transition occurs into another mode of operation with combined capillary flow and free flow outside the capillaries. The axial dry-out is determined by the pressure balance only over that part of the heat pipe where the lack of hydrostatic driving force exists.

REFERENCES

1. J. E. Kemme, J. E. Deverall, E. S. Keddy, J. R. Phillips and W. R. Ranken, Performance tests of gravity-assist heat pipes with screen-wick structures, *Proceedings of the Thermophysics and Heat Transfer Conference*. AIAA/ASME, Boston, MA (1974). AIAA Paper No. 74-723.
2. J. E. Kemme, J. E. Deverall, E. S. Keddy, J. R. Phillips and W. R. Ranken, Temperature control with high performance gravity-assist heat pipes. *Proceedings of the 10th IECEC*, Newark, DE (1975).
3. J. E. Deverall, E. S. Keddy, J. E. Kemme and J. R. Phillips, Gravity-assist heat pipes for thermal control systems. Report LA-5989-MS.
4. J. E. Deverall and E. S. Keddy, Helical wick structures for gravity-assist heat pipes, *Proceedings of the Second International Heat Pipe Conference*, Bologna, Italy (1976), report ESA SP-112, Vol. 1, pp. 3–10 (1976).
5. S. Katzoff, Notes on heat pipes and vapour chambers and their application to thermal control of spacecraft, *Proceedings of The Joint Atomic Energy Commission/Sandia Laboratories Heat Pipe Conference*, Vol. I, pp. 69–89, report SC-M-66-623 (1966).
6. P. Vinz and C. A. Busse, Axial heat transfer limits of cylindrical sodium heat pipes between 25 W/cm^2 and 15.5 kW/cm^2, *International Heat Pipe Conference*, preprints, VDI, Düsseldorf, Paper 2-1 (1973).
7. C. A. Busse, Pressure drop in the vapour phase of long heat pipes, *IEEE Conference Record of the Thermionic Conversion Specialist Conference*, pp. 391–398, Palo Alto, Inst. of Electrical and Electronics Engineers, New York (1967).
8. E. van Andel, Heat pipe design theory, *Proceedings of the Second International Conference on Thermionic Electrical Power Generation*, Stresa 1968, report EUR 4210f, e, pp. 529–542 (1968).
9. C. A. Busse, F. Geiger, D. Quataert and M. Poetzschke, Heat pipe life tests at 1600°C and 1000°C, *IEEE Conference Record of the 1966 Thermionic Conversion Specialist Conference*, pp. 149–158 (1966).
10. J. E. Kemme, Vapour flow consideration in conventional and gravity-assist heat pipes, *Proceedings of the Second International Heat Pipe Conference*, Bologna, Italy, Report ESA SP-112, Vol. 1, pp. 11–22 (1976).
11. C. A. Busse, Theory of the ultimate heat transfer limit of cylindrical heat pipes, *Int. J. Heat Mass Transfer* **16**, 169–186 (1973).
12. T. P. Cotter, Heat pipe startup dynamics, *IEEE Conference Record of the 1967 Thermionic Conversion Specialist Conference*, pp. 344–348. Palo Alto, CA (1967).

APPENDIX 1: INERTIA FORCES IN HEAT PIPE FLOW

For the calculation of the liquid pressure drop in heat pipes it is usual to neglect inertia forces. This is justified if the radial Reynolds number, which is approximately the ratio of inertia

forces over viscous forces, is small compared to one. If the mass flow is equally distributed over N circular liquid flow channels, then [7]

$$Re_r = \frac{1}{2\pi\eta_l L}\frac{1}{N}\frac{dQ}{dz}. \quad (30)$$

As an example let us consider liquid sodium at 800°C. Then $1/2\pi\eta_l L = 0.023$ cm/W. Assuming a linear heating rate of $dQ/dz = 100$ W/cm and a single liquid-flow channel, it follows that $Re_r = 2.3$. The example shows that inertia forces can in fact not always be neglected in liquid pressure calculations especially if there are only very few liquid flow channels.

The action of inertia forces is well known from studies of the vapour flow in heat pipes. Evaluation of equation (30) shows that in the vapour the transition from viscous to inertia flow occurs at fairly low linear heating rates dQ/dz, roughly in the order of 0.1–1 W/cm for non-metallic working fluids and 1–10 W/cm for liquid metals [7]. Heat pipes operating below these limits can conveniently be calculated without consideration of inertia forces. However, care has to be taken not to use corresponding literature formulae beyond the above-mentioned limits; the limited validity of the formulae is unfortunately not always stated.

APPENDIX 2: ENTRAINMENT IN HEAT PIPES

The greatest uncertainty in the flow modelling of heat pipes is actually the question of entrainment, i.e. the stripping of droplets from the menisci in the capillary structure and carrying them with the vapour towards the condenser. Such an extra circulation of mass in addition to the evaporation–condensation cycle would influence the pressure gradient both in the liquid and the vapour and hence the dry-out limit.

The concept of entrainment was already introduced more than 10 years ago by Cotter [12] who drew attention to the dynamic instability of the liquid–vapour interface. If there is an infinite liquid surface with a surface tension γ under gravity-free conditions and vapour of velocity $\bar{w}$ and density ρ flows over this surface, then the amplitude of a small departure from planarity with a wavelength λ will grow exponentially with time if

$$\lambda > \frac{2\pi\gamma}{\rho\bar{w}^2}. \quad (31)$$

The growth of the wave is assumed to lead to stripping of droplets from the crests of the undulations. So equation (31) describes the onset of entrainment from an infinitely large interface under gravity-free conditions. Cotter postulated that this equation would also describe the onset of entrainment from the menisci in a capillary structure. λ would then not be the wavelength of a surface wave, but some function of the capillary geometry.

Now, in a capillary-driven heat pipe the obtainable values of $\rho\bar{w}^2$ are limited by the capillary pressure. From the pressure diagrams in Fig. 2 it is evident that the maximum capillary pressure P_{cm} is certainly larger than only the vapour-pressure drop from inertia forces in the evaporator, which is given by $A\rho\bar{w}^2$ [11]. Hence

$$P_{cm} > A\rho\bar{w}^2. \quad (32)$$

Defining the hydraulic diameter d_h of the capillaries by

$$P_{cm} = \frac{4\gamma}{d_h}, \quad (33)$$

equation (32) can be written as

$$\frac{\gamma}{\rho\bar{w}^2} > \frac{A}{4}d_h. \quad (34)$$

The smallest value for A occurs at the sonic limit and is 1.11 [11]. Herewith from equation (34)

$$\frac{2\pi\gamma}{\rho\bar{w}^2} > 1.74\,d_h. \quad (35)$$

Comparison of equation (35) with the criterion (31) leads to the conclusion that in a capillary-driven heat pipe only waves can grow which have a wavelength λ larger than $1.74\,d_h$, provided that there is an infinitely extended interface for their growth. Such a situation may exist, in a first approximation, if the heat pipe contains surplus liquid and a wet point exists at $z > 0$ as shown in Fig. 2b. An entrainment from the liquid film around z_W would in this case, however, influence only the pressure diagram on the vapour downstream side of the wet point, which is of no concern for the axial dry-out limit. Entrainment can have an effect on the axial dry-out limit only if it occurs on the vapour upstream side of the wet point. This means it has to take place from the single menisci in the capillary structure. Comparing the growth of waves on an infinite surface in a heat pipe and on a meniscus of hydraulic diameter d_h it is difficult to imagine that the capillary structure could do anything else than strongly hinder the growth of waves with $\lambda > 1.74\,d_h$. Therefore it is doubtful whether entrainment may occur from the menisci in a capillary driven heat pipe.

The situation may well be different for gravity-assist heat pipes, where for a given capillary pressure much larger kinetic energy densities can be obtained than given by equation (32) if the hydrostatic driving pressure is large compared with the maximum capillary pressure. Consequently the numerical factor in (35) can be much smaller. For wavelengths $\lambda \ll d_h$, however, one may expect that the damping effect of the capillary structure disappears and entrainment becomes possible.

PHENOMENES D'ASSECHEMENT DANS LES CALODUCS A FLUX CAPILLAIRE ASSISTES PAR GRAVITE

Résumé—Le mécanisme physique est analysé de l'asséchement des caloducs à flux capillaire assistés par gravité. Il est démontré l'existance de deux types opposés d'asséchement. 'L'asséchement axial' a son origine dans le manque de force hydrostatique et apparaît lorsque le flux thermique augmente. Dans le cas de 'l'asséchement azimutal', c'est exactement le contraire. Les relations de base sont dérivées pour l'apparition de ces types d'asséchement. Un exemple explique leur évaluation. Des méthodes sont discutées pour l'empêchement de l'asséchement azimutal. Dans l'appendice on retrouve quelques commentaires critiques sur le rôle des forces d'inertie et d'entraînement dans les caloducs.

AUSTROCKNUNGSERSCHEINUNGEN IN SCHWERKRAFT-UNTERSTÜTZTEN WÄRMEROHREN

Zusammenfassung—Der physikalische Mechanismus des Austrocknens in schwerkraft-unterstützten Wärmerohren wird analysiert. Es wird gezeigt, dass es zwei gegensätzliche Arten des Austrocknens gibt. Das 'axiale Austrocknen' entsteht durch einen Mangel an hydrostatischer Antriebskraft und tritt auf, wenn der Wärmefluss zunimmt. Bei dem 'azimutalen Austrocknen' ist es gerade umgekehrt. Die grundlegenden Beziehungen für das Auftreten dieser Arten des Austrocknens werden hergeleitet. Ihre Auswertung wird an einem Beispeil erläutert. Methoden zur Verhinderung des azimutalen Austrocknens werden diskutiert. Ein Anhang enthält einige kritische Bemerkungen zur Rolle von Trägheitskräften und des Mitreissens von Flüssigkeitströpfchen (Entrainment) in Wärmerohren.

ЭФФЕКТ ОСУШЕНИЯ В ГРАВИТАЦИОННЫХ ТЕПЛОВЫХ ТРУБАХ С КАПИЛЛЯРНЫМ ТРАНСПОРТОМ ЖИДКОСТИ

Аннотация — Анализируется физический механизм явления осушения в гравитационных тепловых трубах с капиллярным транспортом жидкости. Показано наличие двух совершенно противоположных типов данного явления. «Аксиальное осушение» возникает при недостатке гидростатической движущей силы и возрастании плотности теплового потока. В противном случае возникает «азимутальное осушение». Выведены основные соотношения, описывающие возникновение эффекта осушения. На примере показана их оценка. Рассмотрены способы предотвращения возникновения азимутального осушения. Даны некоторые критические замечания о роли сил инерции и уноса в тепловых трубах.